https://doi.org/10.1016/j.apenergy.2019.03.127

This is the Pre-Published Version.

Frequency control of air conditioners in response to real-time dynamic electricity prices in smart grids

Maomao Hu[a,b], Fu Xiao[a,*], John Bagterp Jørgensen[c] and Shengwei Wang[a]

[a] Department of Building Services Engineering, The Hong Kong Polytechnic University, Kowloon, Hong Kong

[b] Research Institute for Sustainable Urban Development, The Hong Kong Polytechnic University, Kowloon, Hong Kong

[c]Department of Applied Mathematics and Computer Science, Technical University of Denmark, DK-2800 Kgs. Lyngby, Denmark

Abstract

In the context of smart grids, residential air conditioners, as the major contributors to home electricity bills and loads on electrical grids, need to be not only energy-efficient, but also grid-responsive to relieve power supply-demand imbalance. Existing demand response control strategies for residential air conditioners focus on single-speed type and mainly adopt temperature set point reset to respond to hourly day-ahead electricity prices. This study represents the first attempt to directly control the operating frequency of inverter air conditioners in response to high-granularity electricity price signals, i.e., 5-minute real-time electricity prices, using model predictive control method. A simplified room thermal model in the stochastic state-space representation and performance maps of an inverter air conditioner are developed and integrated for predicting the coupled thermal response of an air-conditioned room. A demand response-enabled model predictive controller is designed based on the coupled model to optimally control the operating frequency of the inverter air conditioner while taking account of all the influential variables including weather conditions, occupancy, and 5-min real-time electricity prices. A Kalman filter is adopted to estimate the unmeasurable variables and remove the noises in measurements. A TRNSYS-MATLAB co-simulation testbed is developed to test the thermal and energy performances of the model predictive controller. Results show that compared to the PID controller, the demand response-enabled model predictive controller can implement

* Corresponding author. Tel.: +852 2766 4194; Fax: +852 2765 7198

E-mail address: linda.xiao@polyu.edu.hk

© 2019. This manuscript version is made available under the CC-BY-NC-ND 4.0 license https://creativecommons.org/licenses/by-nc-nd/4.0/.

automatic and optimal precooling to improve occupant's thermal comfort at the beginning of occupancy. Moreover, it can also reduce average power consumption during peak demand periods by 17.31% to 38.86% compared with the PID controller and reduce all-day electricity costs by 0.42% to 22.16%. The frequency-based model predictive control method enables residential inverter air conditioners to be more grid-friendly and cost-efficient.

Keywords: Inverter air conditioners; Model predictive control; Real-time electricity prices; Gray-box room thermal model; Demand response; Smart grid.

Nomenclature

A	area, m^2
A	system matrix in state-space model
AC	air conditioner
B	input matrix in state-space model
C	equivalent overall thermal capacitance, J/K
C	output matrix in state-space model
DAP	day-ahead electricity pricing
DR	demand response
E	disturbance matrix in state-space model
e	slack variable
ERCOT	Electric Reliability Council of Texas
GA	genetic algorithm
HVAC	heating, ventilation and air conditioning
MIMO	multiple-input multiple-output

MPC	model predictive control
N	operating frequency of compressor motor, Hz
N	prediction horizon
P	power consumption, W
P	covariance matrix of state estimate error
PID	proportional–integral–derivative control
Q	cooling capacity of AC, W
Q	heat gains, W
Q	covariance matrix of process noise
R	equivalent overall thermal resistance, K/W
R	covariance matrix of measurement noise
RC	resistance-capacitance room thermal model
RMSE	root mean square error
RTP	real-time electricity pricing
T	temperature, ℃
TMY	typical meteorological year
TRN	TRNSYS
v	measurement noise
w	process noise

y	observed output vector in state-space model

Greek symbols

ρ	penalty to the slack variable

Subscripts

comp	Compressor
cp	cumulative probability
d	discrete-time
ext	external surface of wall
in	indoor air
int	internal surface of wall
inter	internal heat gains
k	sampling time step
lb	lower bound
m	internal thermal mass
max	Maximum
o	outdoor air
solar	heat gain from solar radiation
thsh	Threshold
ub	upper bound

w	Wall
win	Window

1. Introduction

The increasing penetration of renewable energy resources at supply side and plug-in electric vehicles at demand side are exacerbating the power imbalance in today's electrical grids. The power imbalance will result in the severe consequences in terms of the power quality and reliability, such as voltage fluctuations and even power outages. Demand response (DR) has been considered as an effective and promising solution to the power imbalance issue in recent years, which refers to changes in electric usage made by end-users in response to changes in the electricity prices over time when system reliability is jeopardized [1]. Buildings, as the major end users of electricity, have great potential to provide peak power reductions and to improve the grid reliability. As the Federal Energy Regulation Committee reported, residential buildings would provide the greatest DR potential and the residential customers would be able to provide more than 45% of the total potential DR resources in 2019 [2]. Many studies have focused on DR management of residential ACs, and optimal scheduling of the indoor air temperature set points is a common DR control method for residential ACs.

During the optimal scheduling, dynamic electricity prices from electric utilities were usually considered in the objective function to minimize the all-day electricity cost while still satisfying the occupant's thermal comfort. The optimal scheduling usually involves two major tasks: development of the thermal response model of an air-conditioned room and the optimization problem formulation and solving. Chen et al. [3] optimized the on/off schedule of home electrical appliances by using stochastic and robust optimization methods. A simplified one-order model was used to describe the relationships among indoor air temperature, out air temperature, and energy consumption of AC. Hubert et al. [4] formulated a mixed-integer linear programming problem, which was solved using GUROBI software, to minimize the electricity cost by on/off control of the AC. The air-conditioned room was modeled as a three-order thermodynamic system. Li et al. [5] used a heuristic method and particle swarm optimization to schedule the optimal set points of the indoor air temperature for on/off control of ACs. The operating costs under various dynamic electricity prices and environmental conditions were compared with the assistance of the eQUEST simulation. Thomas et al. [6] developed

an intelligent AC controller that can provide the end-use customers with optimal trade-offs between comfort and cost by scheduling the on/off status of AC. A two-order equivalent thermal parameter model was used to represent the room thermal dynamics. Some other algorithms were used for energy consumption forecasting and energy dispatch, such as backtracking search algorithm [7], artificial cooperative search algorithm [8], and optimized gene expression programming [9]. Most residential ACs concerned in the previous studies were single-speed ACs with on-off control.

However, on-off control carries the great disadvantage of undesired current peaks during state transitions [10]. Meanwhile, single-speed ACs are also being gradually replaced by inverter ACs, which have greater energy efficiency in partial-load conditions. Inverter ACs can operate within a wide range of frequencies (20 to 100 Hz), which is accompanied by large variations in power consumption. The control algorithms of inverter ACs are more complicated than those of single-speed ACs. Besides, previous studies on DR control of residential appliances mainly targeted at day-ahead electricity prices (DAPs), which are at hourly intervals and usually announced to the end-users one day ahead at midnight, rather than real-time electricity prices (RTPs), e.g., the high-granularity RTPs at 5-min intervals [11]. Three challenging issues remain to be addressed in response to real-time electricity prices. First, the dynamics of the indoor air temperature is much slower than the response of an AC due to thermal mass of the building. As a result, the indoor air temperature could not track the frequently changed set points when the temperature set points are adjusted every 5 minutes. It means the conventional DAP-based optimal scheduling of the temperature set points doesn't work well with 5-minute RTPs. Second, computation load becomes critical in responding to RTPs because of the shorter interval of the changes of electricity prices. The sophisticated modeling and optimization techniques used in DAP-based DR strategies may not be suitable for RTP-based DR strategies. Third, for inverter ACs, direct control of the compressor frequency, which largely determines the AC power consumption, is more effective in responding to RTPs every 5 minutes and regulating power consumption. Therefore, a new frequency-based DR control method is needed for residential inverter ACs to respond to 5-min RTPs and it is the research focus of the present study.

Model predictive control (MPC) is a promising method for frequency-based DR control of residential inverter ACs in response to 5-min RTPs. It is an intuitive and well-established approach for constrained control, which was initially applied in the process industries, such as petroleum refineries

and chemical plants, in the late 1970s [12]. It has received increasing and extensive research interests in the field of building and HVAC system control in the last decade. Both experimental [13, 14] and simulation [15, 16] attempts have been made to apply MPC method to building environmental control. According to different control goals and optimization functions, they can be categorized into: maximizing occupants' thermal comfort [17, 18]; minimizing total energy consumptions [13, 19], operational costs [20, 21], or greenhouse gas emissions [22]; minimizing peak load demands [23, 24]; and maximization of the productivity of renewable energy sources [25, 26]. MPC is particularly suitable for frequency-based DR control of inverter ACs because it can output optimal operating frequency while simultaneously considering all the influential factors including weather conditions, occupancy and 5-min RTPs.

This paper presents a novel MPC-based frequency control method for inverter ACs, which directly control the operating frequency of compressor in response to 5-minute RTPs. The present study is an extension of our previous work [27], in which we developed a model-based optimal control method for inverter ACs in response to hourly DAPs. Specifically, we make new contributions in two respects. First, we develop a computationally efficient simple-structured room thermal model in the stochastic state-space form for MPC. The state-space model is chosen because it is beneficial to formulate a convex and easily solved optimization problem. Random white noise is added to the model to make it more realistic. Second, we develop a novel DR-enabled MPC controller to directly control the operating frequency of inverter ACs in response to high-granularity electricity prices, i.e. 5-min RTPs. The proposed DR-enabled MPC controller enables the inverter AC to be price-responsive and grid-interactive and can efficiently reduce power consumptions during peak demand periods and reduce electricity costs without sacrificing thermal comfort. A Kalman filter is used to estimate the unmeasurable variables and to filter the noises in measurements. To the best of our knowledge, the proposed frequency-based MPC controller in this work is the first of its kind for DR control of residential inverter ACs to provide quick response to the 5-minute RTPs.

The remainder of this paper is organized as follows. Section 2 introduces the general implementation structure of the proposed MPC method for inverter ACs. The development and validation of offline data-driven system models are presented in Section 3. The proposed online MPC methods are introduced in Section 4. In Section 5, we test and compare the performances of the integrated building

energy system under on-off controller, PID controller and two types of MPC controllers on the TRNSYS-MATLAB co-simulation testbed. Finally, our conclusions are presented in Section 6.

2. Overview of the proposed MPC method for residential inverter ACs

Before the development of MPC controllers for inverter ACs is described, the fundamentals behind MPC are briefly discussed in this section. MPC is an advanced control method that can systematically take account of future predictions during the control design stage while satisfying the system operating constraints. The main idea is to use system models to predict the evolution of the system under the predicted operating conditions. During each sampling interval, beginning at the current state, an optimal control problem is formulated and solved over a finite horizon. MPC is intrinsically a feedback control that incorporates iterative optimizations over moving prediction horizons. The optimization result is a trajectory of future control inputs into a system that satisfy the system dynamics and time-varying constraints. However, only the first control signal is adopted by the system at the next sampling time, whereas the rest of the sequence is discarded. At the following time step, the optimization is repeated based on the updated current state over the next prediction horizon.

The formulations of cost function, system dynamics, and constraints play significant roles in the performance of an MPC scheme. To obtain simple optimization problems, most cost functions that describe desired performance are convex, such as quadratic costs and linear costs. Instead of using the concept of a specific set point for the controlled variables, the specified constraints of the optimization problem are chosen to fulfill the control targets. A range of constraints, including linear constraint, convex quadratic constraint, switched constraint, and nonlinear constraint, are used in practice. Due to the computational simplicity, linear constraint is the most common type of constraint, in which the upper and lower bounds of variables are normally used as optimization constraints. The system dynamic model, as the cornerstone of the MPC, is used to predict the future system outputs. They are usually represented in the forms of impulse response, step response, transfer function, and state space. For multiple-input multiple-output (MIMO) systems, the state space model is commonly used [16] to describe system dynamics. Moreover, the state space model can be used to formulate convex and easily solved optimization problems.

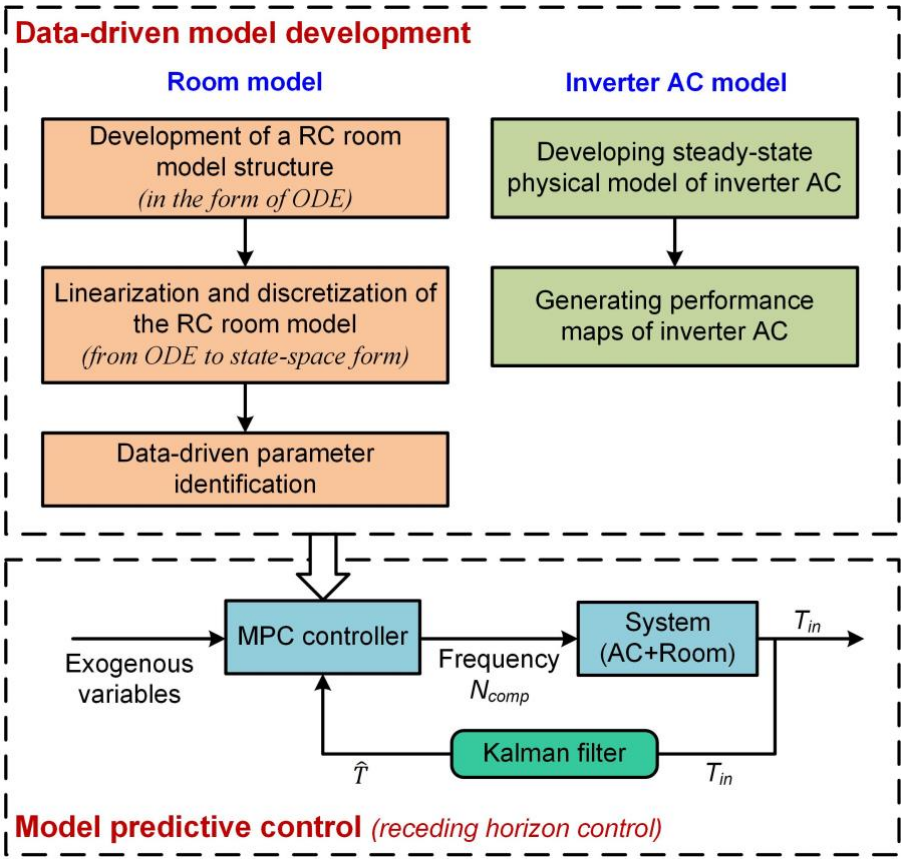

Fig. 1. Block diagram of implementation structure of MPC for inverter ACs.

The implementation structure of MPC for inverter ACs, as shown in Fig. 1, includes two main parts: offline data-driven model development and online MPC. The system of interest in this study is an integrated building energy system that includes an air-conditioned room and an inverter (variable-speed) AC. Considering the computational efficiency for online MPC-based DR control, control-oriented models of both the room and the inverter AC are required. In this study, we develop a stochastic state-space model of room thermal dynamics and 3-dimensional performance maps of inverter ACs, based on the detailed physical models developed in our previous work [27], for online prediction of the system's evolution under the influence of predicted future exogenous variables such as weather conditions, occupancy, and RTP. The output of the MPC controller is the control signal of operating frequency of the AC, which is used to control the compressor speed directly.

3. Development of data-driven model for online MPC

System modeling consumes the largest portion of time in the process of developing an MPC controller, typically around 80% in the industrial process field [28] and 60% in the built-environment field [29]. MPC of inverter ACs in response to 5-minute RTP requires fast and accurate dynamic models. To

balance model accuracy and computational efficiency, we adopted a general approach to develop models (i.e., from relatively detailed models with sophisticated physical meanings to simplified data-driven models).

3.1. Room thermal model

3.1.1. Model development

The building models in commonly used simulation software such as TRNSYS, EnergyPlus, and eQUEST cannot be readily used for model-based control methods because they are complex and usually time-consuming. In previous studies [30], we developed, identified, and validated a gray-box RC room thermal model. The structure of the gray-box model is illustrated in Fig. 2. The gray-box room thermal model can learn the thermal characteristics of the to-be-controlled room by analyzing the data collected from smart in-home sensors. Due to the simplicity of the model structure, the developed room thermal model can be easily integrated in the model-based controller to effectively predict the room's thermal dynamics. The energy balance for the external and internal walls, indoor air, and internal thermal mass are given by Eqs. (1) - (4).

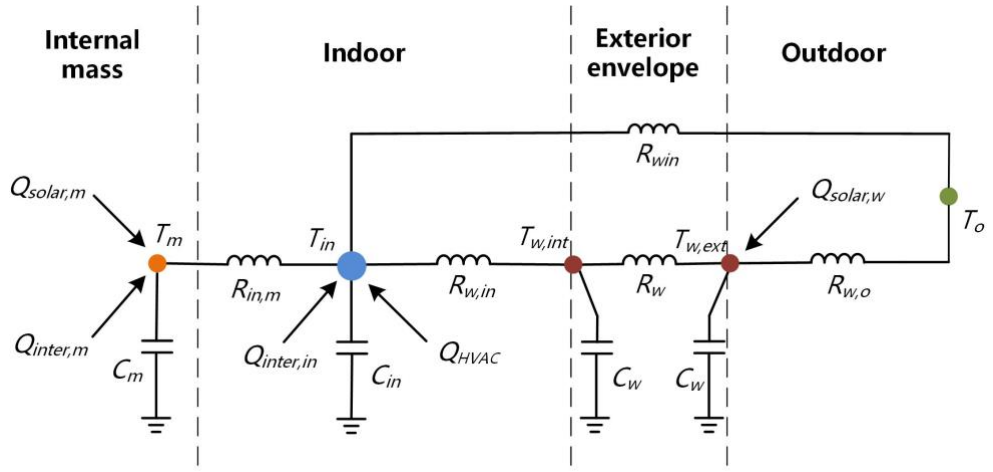

Fig. 2. Schematic of the gray-box RC room thermal model.

$$C_w \frac{dT_{w,ext}}{dt} = \frac{T_o - T_{w,ext}}{R_{w,o}} + \frac{T_{w,int} - T_{w,ext}}{R_w} + f_{solar,w} A_w I_{solar} \quad (1)$$

$$C_w \frac{dT_{w,int}}{dt} = \frac{T_{w,ext} - T_{w,int}}{R_w} + \frac{T_{in} - T_{w,int}}{R_{w,in}} \quad (2)$$

$$C_{in} \frac{dT_{in}}{dt} = \frac{T_m - T_{in}}{R_{in,m}} + \frac{T_{w,int} - T_{in}}{R_{w,in}} + \frac{T_o - T_{in}}{R_{win}} + f_{inter,in} Q_{inter} + Q_{HVAC} \quad (3)$$

$$C_m \frac{dT_m}{dt} = \frac{T_{in} - T_m}{R_{in,m}} + f_{solar,m} A_{win} I_{solar} + f_{inter,m} Q_{inter} \quad (4)$$

where R and C represent the overall heat resistance and capacitance; T denotes temperature; the subscripts *in, o, w, int, ext, win,* and *m* indicate indoor air, outdoor air, exterior wall, internal wall surface, external wall surface, window, and internal mass, respectively; Q_{inter} denotes the internal heat gain, I_{solar} denotes the global solar radiation, A denotes the geometric area, and f denotes the conversion coefficients for the heat gains, which are also identified together with R and C. The detailed model identification methods can be found in our previous publication [30].

3.1.2. Model linearization and discretization

The dynamic room thermal model, as described by differential equations (1) – (4), is an MIMO system. State space models are commonly used to model MIMO systems because of their advantage in explicit expression of the relationships between the outputs and inputs. They can also be used to formulate convex optimization problems that can generally be solved conveniently with state-of-the-art optimization techniques. To make the model more realistic, white Gaussian noise is added into the system model. Eqs. (1) – (4) can be converted into a continuous-time state-space model with stochastic noise, as shown in Eq. (5).

$$dT = (AT + Bu + Ed)dt + dw(t) \tag{5}$$

Where the system state $T = [T_{w,ext} \quad T_{w,int} \quad T_{in} \quad T_m]^T$; the input vector $u = Q_{HVAC}$; the disturbance vector $d = [T_o \quad I_{solar} \quad Q_{inter}]^T$; the system matrix $A =$

$$\begin{pmatrix} \frac{-1}{C_w R_{w,o}} + \frac{-1}{C_w R_w} & \frac{1}{C_w R_w} & 0 & 0 \\ \frac{1}{C_w R_w} & \frac{-1}{C_w R_w} + \frac{-1}{C_w R_{w,in}} & \frac{1}{C_w R_{w,in}} & 0 \\ 0 & \frac{1}{C_{in} R_{w,in}} & \frac{-1}{C_{in} R_{w,in}} + \frac{-1}{C_{in} R_{in,m}} + \frac{-1}{C_{in} R_{win}} & \frac{1}{C_{in} R_{in,m}} \\ 0 & 0 & \frac{1}{C_m R_{in,m}} & \frac{-1}{C_m R_{in,m}} \end{pmatrix}_{4\times4}$$

; the input matrix $B = (0 \quad 0 \quad 1/C_{in} \quad 0)^T$; the disturbance matrix $E =$

$$\begin{pmatrix} \frac{1}{C_w R_{w,o}} & \frac{f_{solar,w} \times A_w}{C_w} & 0 \\ 0 & 0 & 0 \\ \frac{1}{C_{in} R_{win}} & 0 & \frac{f_{inter,in}}{C_{in}} \\ 0 & \frac{f_{solar,m} \times A_{win}}{C_m} & \frac{f_{inter,m}}{C_m} \end{pmatrix}_{4\times3}$$

; $w(t)$ is a Wiener process, which is a stochastic process with independent normal distributed increments.

In practical applications, the stochastic continuous-time state-space model needs to be discretized, and the stochastic discrete-time state-space model is given by Eqs. (6) and (7).

$$T_{k+1} = A_d T_k + B_d u_k + E_d d_k + w_k \quad (6)$$

$$y_k = C_d T_k + v_k \quad (7)$$

where A_d, B_d, and E_d are the corresponding matrices of the discrete-time state-space model, which depend on the sampling time. The observed output vector $y_k = T_{in}$; and the output matrix $C_d = (0 \quad 0 \quad 1 \quad 0)$. The random variables w_k and v_k represent the process and measurement noises, respectively, which are assumed to be independent and white and to have normal distribution probabilities (i.e., $w_k \sim N(0, Q)$ and $v_k \sim N(0, R)$). Q and R are the covariance matrices of the process noise and the measurement noise, respectively. Eqs. (6) and (7) are used in the MPC controller to online predict the system evolution.

3.1.3. Identification of model parameters

A prototype room in a residential flat in Hong Kong is modeled in TRNSYS. The residential room (L × W × H: 4.8 × 3.6 × 3 m) has one south-facing exterior wall (3.6 × 3 m) and one east-facing exterior wall (4.8 × 3 m). Both exterior walls have single glazed windows and the window-wall-ratio of each wall is 0.2. The overall heat transfer coefficients of the exterior wall and the single glazed window are 2.57 and 5.69 W/(m^2·K), respectively. Instead of using the default TMY weather data, real historical weather data at 1-minute intervals from the Hong Kong observatory are used in simulation tests. Four weeks (1 June to 29 June 2015) of indoor air temperature data at 1-minute intervals generated from TRNSYS are used to identify the room thermal model. The identification results are as follows: C_w = 8,381,606 J/K, C_{in} = 871,887 J/K, C_m = 13,904,351 J/K, R_{win} = 0.0051 K/W, R_w = 0.0060 K/W, $R_{w,o}$ = 0.0010 K/W, $R_{w,in}$ = 0.0041 K/W, $R_{in,m}$ = 0.0023 K/W, $f_{solar,w}$ = 0.4834, $f_{solar,m}$ = 0.0012, $f_{inter,in}$ = 3.0367, and $f_{inter,m}$ = 0.9976. Fig. 3 shows the outdoor air temperatures, solar radiation, and indoor air temperature generated from TRNSYS ($T_{in,TRN}$) and the RC model ($T_{in,RC}$). The results show that the RC room thermal model can predict the indoor air temperature with a relatively high degree of accuracy.

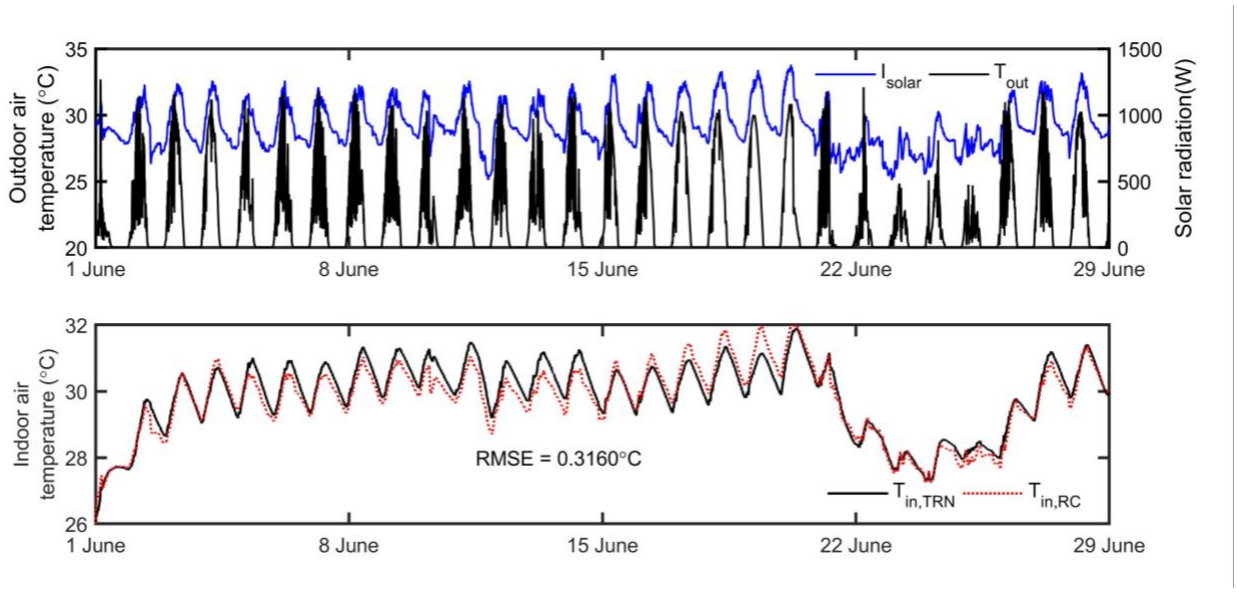

Fig. 3. Weather conditions and indoor air temperature generated from TRNSYS and the RC model.

With the identified RC values and a 5-minute sampling interval, the matrices in the discrete-time state-space model (i.e., Eqs. (6) and (7)) can be determined as follows:

$$A_d = 10^{-2}\begin{pmatrix} 95.809 & 0.5757 & 0.0023 & 0.0001 \\ 0.5757 & 98.573 & 0.7543 & 0.0600 \\ 0.0223 & 7.2508 & 73.899 & 13.012 \\ 0.0001 & 0.0362 & 0.8159 & 99.119 \end{pmatrix}_{4\times4}; \quad E_d = 10^{-4}\begin{pmatrix} 361.21 & 3.4146 & 0.0001 \\ 3.7494 & 0.0101 & 0.0415 \\ 581.53 & 0.0004 & 9.0293 \\ 2.8933 & 0.0013 & 0.2591 \end{pmatrix}_{4\times3};$$

$B_d = 10^{-5}(0.0003 \quad 0.1367 \quad 29.686 \quad 0.1477)^T$; $C_d = (0 \quad 0 \quad 1 \quad 0)$.

3.2. Performance maps of an inverter AC

AC models are generally classified into transient and steady-state models. The refrigerant dynamics in residential ACs are much quicker than the room's thermal dynamics. The redistribution of refrigerant throughout the various AC components normally requires only around 100 seconds. Therefore, a steady-state AC model can predict the coupled dynamic behaviors of the room and the AC under time-varying internal and external conditions. However, for online MPC-based DR control in response to 5-minute RTP, the computation time of the detailed steady-state model is unaffordable. Therefore, we develop 3-dimensional performance maps of inverter ACs based on the steady-state inverter AC models developed in our previous work [27]. The model of inverter ACs was validated using the experimental data of a Mitsubishi split-type inverter AC. The rated cooling capacity of the tested inverter AC is 2.5 kW.

Performance map is a kind of graphical representation designed to show the performances of a system at different levels of disturbances. Since the performance of inverter ACs is quantified by both its cooling capacity and COP, the performance maps of inverter-driven ACs include the cooling capacity map and the COP map. The typical operating conditions are the combinations of different compressor rotational speeds (N_{comp} = [*20, 30,…, 100*]), indoor air temperature (T_{in} = [*21, 24, 27, 30, 33, 36*]) and outdoor air temperature (T_{out} = [*23, 26, 29, 32, 35, 38*]). The performance data of the inverter AC under the typical operating conditions are obtained from simulation tests conducted using the steady-state inverter AC model developed in our previous work. With the performance maps, the cooling capacities and COP of the inverter AC at given indoor and outdoor conditions and compressor frequencies can be obtained by 3-dimensional interpolations.

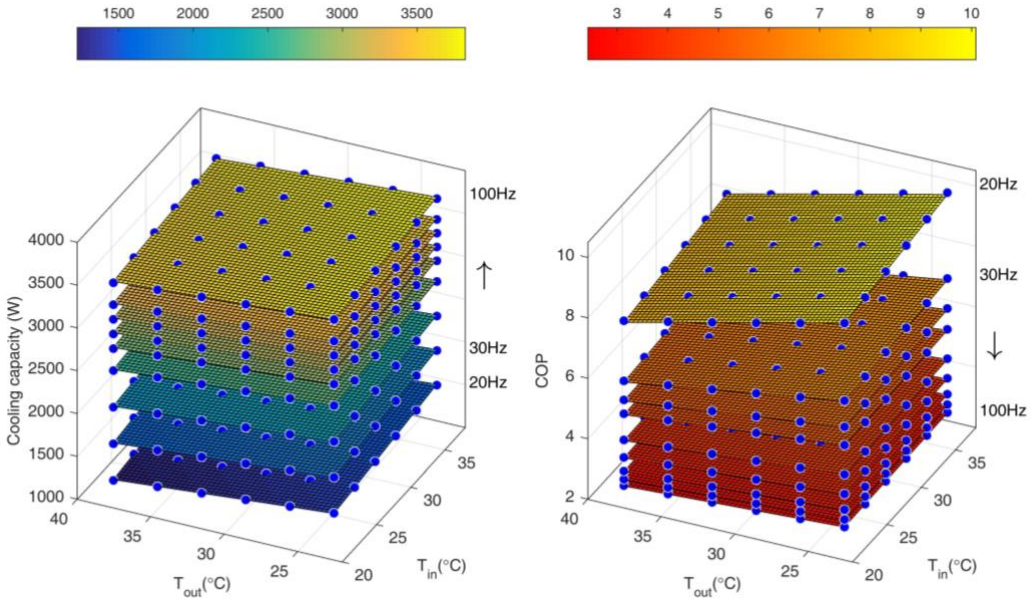

Fig. 4. Performance maps (cooling capacity and COP map) of the inverter AC at a range of compressor speeds.

Fig. 4 shows the performance maps of the inverter AC at a range of compressor speeds, i.e., 20-100Hz. It can be found that the cooling capacity increases as the compressor speed increases, but the COP decreases as the compressor speed increases. The outdoor air temperature has a greater influence on the COP than the indoor air temperature. The performance maps of the inverter AC under the full range of operating conditions are used for online MPC in this study.

4. Online model predictive control

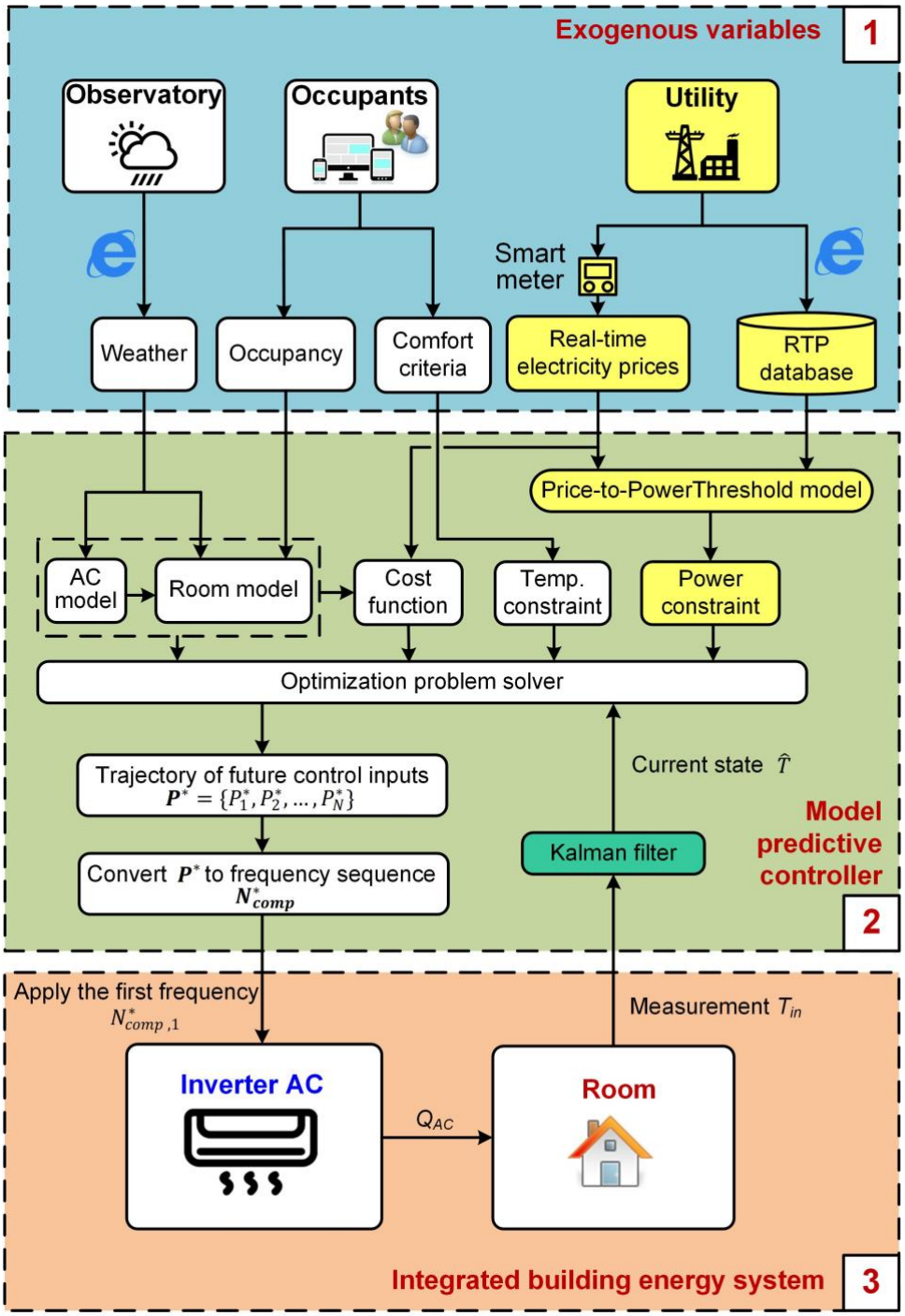

Fig. 5. Flow chart of online model predictive control for inverter ACs.

For purposes of comparison, two types of MPC controllers are designed for inverter ACs: a DR-enabled MPC controller with automatic response capability to RTP and an ordinary MPC controller without DR function. Three major steps are included in each time step of MPC, as shown in Fig. 5: (1) preparation/prediction of the exogenous input variables, including the weather, occupancy, and RTP; (2) solution of the optimization problem based on the predicted exogenous inputs and updated

current state filtered by the Kalman filter; and (3) control implementation and measurement. Fig. 5 illustrates the flows of both the DR-enabled MPC controller and the ordinary MPC controller without DR function. The RTP-related blocks (in yellow) are involved only in the DR-enabled MPC controller.

4.1. Preparation/prediction of exogenous input variables

4.1.1. Weather conditions and occupancy

Weather conditions, such as the outdoor air temperature and the solar radiation, influence a room's thermal dynamics and AC performance; these data may come from a local observatory or from prediction models [31]. The integrated building energy system model used in the MPC controllers in this study makes predictions regarding system dynamics based on local weather forecasts. Occupancy prediction plays a significant role in model-based building climate control. The occupancy pattern determines the internal heat gain and the control range of the indoor air temperature over the prediction horizon. In practical implementation, occupancy information can either be preset by the customers or obtained from smart mobile devices and Internet of Things devices [32]. In our simulation studies, the real-time weather forecast is obtained from the local observatory website, and the occupancy is pre-specified for the sake of simplicity.

4.1.2. RTP and dynamic power thresholds

The typical RTP at 5-minute intervals is considered in the development of the DR-enabled MPC controller for inverter ACs. Fig. 6 shows the historical nodal dynamic RTPs of the Electric Reliability Council of Texas (ERCOT) in June 2016 [33] to illustrate the large daily fluctuations in typical daily RTP profiles.

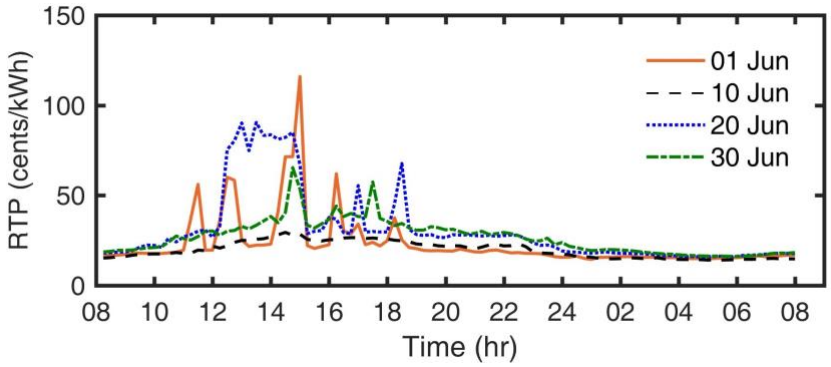

Fig. 6. Daily RTP profiles in the ERCOT retail market on typical days of June 2016.

To achieve supply-demand balance in electrical grids, grid operators usually increase the RTP to prompt DR program participants to reduce power consumption during peak demand periods. To obtain effective responses, a power constraint based on dynamic pricing is usually adopted in DR control methods for residential appliances. When the RTP is high, a low operating power threshold can be set for electric appliances to provide DR resources and reduce operating costs. In a similar way, when the RTP is low, a high operating power threshold can be adopted. Based on this idea, a "Price-to-Power Threshold" model for inverter ACs is formulated in this study. The cumulative probability distribution of RTP, which is obtained by analyzing the historical RTP database, can help us develop the model. The cumulative probability of RTP refers to the likelihood that the RTP is less than or equal to a specified value of RTP. Fig. 7 shows the probabilities and cumulative probability distribution of RTPs in the ERCOT retail market in June 2016. Taking as an example the point denoted by the triangle symbol in Fig. 7-b, the cumulative probability is explained here. The point (24.97, 70%) means that the probability is 70% when the RTP is 24.97 cents/kWh or less (i.e., $RTP_{cp=0.7} = 24.97$).

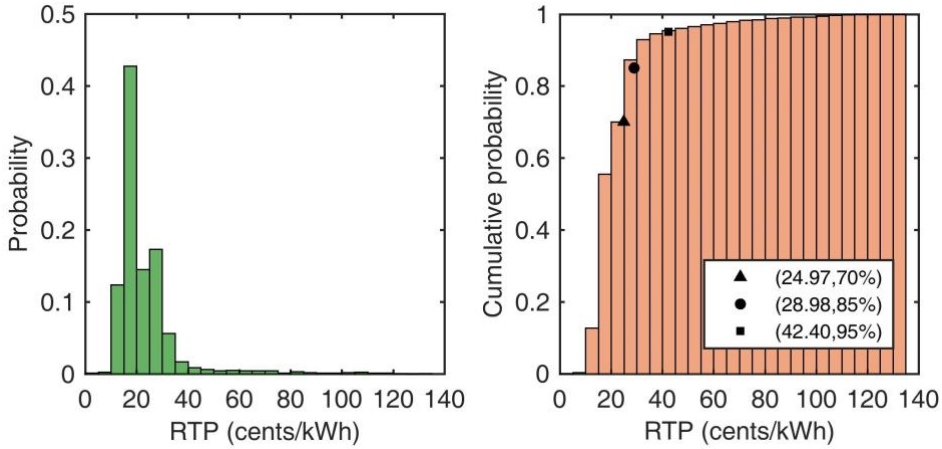

Fig. 7. (a) Probabilities and (b) cumulative probability distribution of RTPs in the ERCOT retail market in June 2016.

Using the cumulative probability distribution of RTP, we propose a scheme to determine dynamic power thresholds for the DR-enabled MPC control that can be mathematically described by Eq. (16).

$$P_{thsh,i} = \begin{cases} 100\% \cdot P_{max} & \text{if } RTP_i \le RTP_{cp=0.7} \\ 85\% \cdot P_{max} & \text{if } RTP_{cp=0.7} < RTP_i \le RTP_{cp=0.85} \\ 70\% \cdot P_{max} & \text{if } RTP_{cp=0.85} < RTP_i \le RTP_{cp=0.95} \\ 55\% \cdot P_{max} & \text{if } RTP_i \ge RTP_{cp=0.95} \end{cases} \tag{16}$$

where P_{max} refers to the maximum operating power of an inverter AC; $P_{thsh,i}$ denotes the dynamic power threshold at time step i; and $RTP_{cp=0.7}$, $RTP_{cp=0.85}$, and $RTP_{cp=0.95}$ are the RTPs when the cumulative probabilities (cp) are 0.7, 0.85, and 0.95, respectively. The dynamic power thresholds are used as a time-varying constraint in the DR-enabled MPC controller to limit the maximum operating power of AC during peak demand periods.

4.2. Formulation and solving of optimization problem

For purposes of comparison, a DR-enabled MPC controller and an ordinary MPC controller without DR function are developed in this study to fulfill different tasks. A general MPC framework includes four parts: cost function, constraints, system dynamics, and current state [16]. The difference between the two MPC controllers is the construction of cost function and constraints.

4.2.1. DR-enabled MPC controller responding to RTP

The objective of the DR-enabled MPC controller is to minimize the operating costs of the inverter AC over the prediction horizon N while keeping the indoor air temperature within a pre-specified range. The optimization problem is formulated as Eqs. (17) - (22).

$$\min_{P_1,P_2,\ldots,P_{N-1}} \sum_{k=1}^{N-1} P_k \Delta t \cdot RTP_k + \rho_e e_k \tag{17}$$

subject to

$$T_{k+1} = A_d \cdot T_k + B_d \cdot COP_k \cdot P_k + E_d \cdot d_k + w_k \tag{18}$$

$$y_k = C_d T_k + v_k \tag{19}$$

$$y_{lb,k} - e_k \le y_k \le y_{ub,k} + e_k \tag{20}$$

$$e_k \ge 0 \tag{21}$$

$$P_k = 0 \text{ or } P_{min} \le P_k \le P_{thsh,k} \tag{22}$$

where N is the prediction horizon; Δt is the prediction interval; P_k and COP_k are the AC power consumption and COP at time step k, respectively; $P_{thsh,k}$ is the dynamic power threshold; T_k, y_k, and d_k are the state vector, output vector, and disturbance vector in the state-space system model, respectively; w_k and v_k are the process and measurement noise, respectively, which are assumed to be independent and white and to have a normal distribution. A_d, B_d, C_d, and E_d are the state-space matrices of the discrete-time state-space model.

The objective function, Eq. (17), aims to minimize the operating costs over the prediction horizon. If the constraints are not violated, the optimal power consumption remains at 0 kW, i.e., the AC is turned off. Eqs. (18) - (19) depict the system dynamics in a state-space form. The input variable, the cooling capacity ($Q_{HVAC,k}$), is obtained by the product of COP_k and power consumption (P_k). Eq. (20) is a dynamic soft constraint that maintains the indoor air temperature within a certain range. During unoccupied hours, it is supposed that the AC is turned off and that the optimized power consumption is 0 kW. To achieve that goal, a wide temperature range is normally set, e.g., 20℃ to 30℃, as a result, the indoor air temperature is always within the range and AC remains off during the unoccupied period. When the room is occupied, a narrow temperature range is set to ensure thermal comfort (i.e., 22°C to 24°C when the occupants are awake and 24°C to 26°C while the occupants sleep). However, the temperature constraint may not be satisfied in practice even if the AC runs at its full cooling capacity, such as on an extremely hot day. This situation may lead to a failure to solve the optimization problem. To address this issue, we can relax the MPC problem by introducing a slack variable e_k. The hard constraint is then converted to a soft constraint, which has a similar function as the dead-band plays in the on-off control. To ensure that the preset temperature range is met most of the time (i.e., $e_k = 0$), an especially large penalty ρ_e can be imposed on the slack variable e_k in the objective function. Eq. (22) is a time-varying hard constraint to limit the maximum power consumption of AC based on the RTP from electric utilities. An inverter AC has a minimum operating frequency (e.g., 20 Hz) and corresponding minimum power consumption P_{min}. Therefore, the power consumption should range between P_{min} and $P_{thsh,k}$, which can be determined by Eq. (16) or equal zero when it is turned off.

The prediction horizon N and prediction interval Δt play significant roles in MPC controllers. The optimal prediction horizon is a trade-off between the accuracy of the predictions of exogenous inputs and a sufficient length of the prediction horizon. A long horizon also increases the computation time for each optimization step. For the MPC of radiant heating systems, the prediction horizon is normally set as 6 to 48 hours because the rooms have large thermal masses and respond very slowly to the heating system [13, 34-37]. However, the room concerned in this study is located in a cooling-dominated district and has a relatively small thermal mass. In addition, the inverter AC delivers cooling to the space via heat convection, which is a direct and quicker mode of heat transfer than heat radiation in a radiant heating system. Considering the short thermal response time of the target room

to the cooling system, the prediction horizon *N* in this study is set to 3 hours, which is sufficient for the inverter AC to respond in advance to upcoming disturbances. The prediction interval is the frequency at which the optimization problem is solved and at which the actuator receives the control signal. Considering the room's thermal response time and the compressor motor's life expectancy, the compressor's rotational speed is allowed to change every 5 minutes (i.e., the prediction interval of the MPC controller in our study is 5 minutes).

4.2.2. Ordinary MPC controller without DR function

Compared with the DR-enabled MPC controller, the ordinary MPC controller without DR function does not consider the dynamic RTP in formulating the optimization problem. The optimization problem of the ordinary MPC scheme, which aims to save the energy use, can be described by the objective function Eq. (23), and the constraints including Eqs. (18) - (21) and Eq. (24). In contrast to the time-varying constraint (Eq. (22)), in the DR-enabled MPC controller, Eq. (24) is a static constraint that limits power consumption in a constant power range.

$$\min_{P_1,P_2,\ldots,P_{N-1}} \sum_{k=1}^{N-1} P_k \Delta t + \rho_e e_k \tag{23}$$

$$P_k = 0 \text{ or } P_{min} \le P_k \le P_{max} \tag{24}$$

4.2.3. Current state estimation using the Kalman filter

At the beginning of each optimization step, the current state is needed as the starting point for optimization. In our case, the system state includes four variables: $T = [T_{w,ext} \quad T_{w,int} \quad T_{in} \quad T_m]^T$. However, only the indoor air temperature T_{in} is measured in real applications. To address this issue, the Kalman filter is commonly used to estimate the immeasurable variables and to filter the noise in measurements [38, 39]. The Kalman filter is an algorithm that provides a computationally efficient solution to estimate the state of a process in a manner that minimizes the prediction mean squared error. The solution is recursive in such a way that each updated estimate of the state is computed from the previous estimate and the new measured data. As shown in Fig. 8, each Kalman filter cycle includes two steps: time update (priori estimate) and measurement update (posteriori estimate). *P*, *Q*, and *R* are the covariance matrices of the state estimate error, the process noise, and the measurement noise, respectively. $\hat{T}_k'$ denotes a priori state estimate at time step k. $\hat{T}_k$ denotes the posteriori state

estimate given measurement y_k (i.e., indoor air temperature T_{in}) at time step k. K_k is the Kalman gain determined by solving an algebraic Riccati equation. I is an identity matrix.

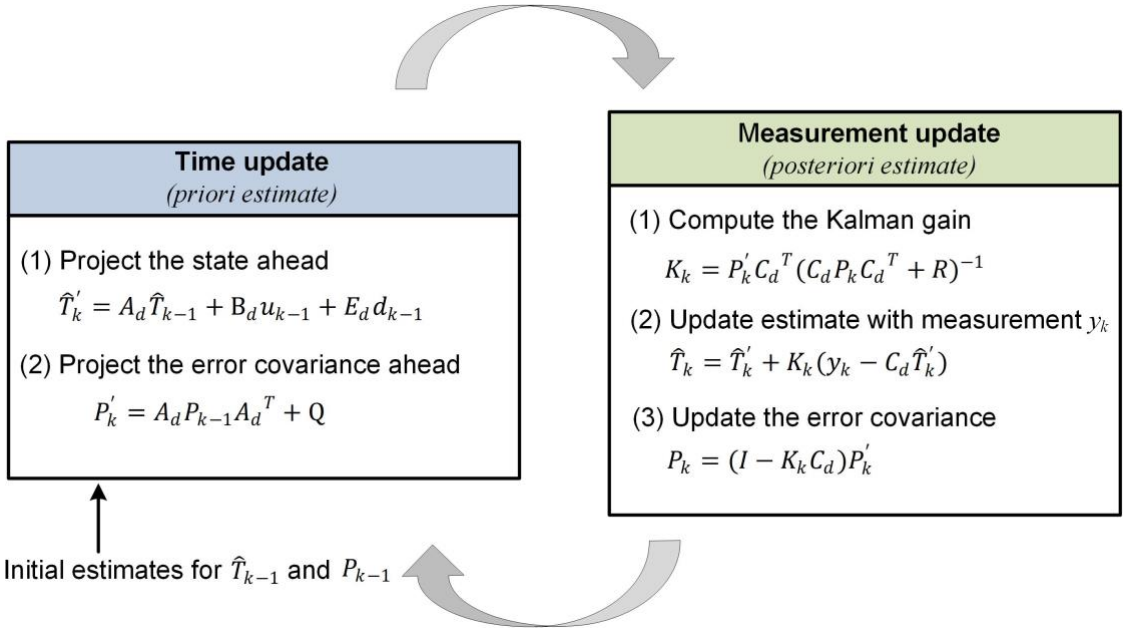

Fig. 8. Kalman filter cycle for current state estimate in MPC.

4.3. Implementation of frequency signal from MPC controllers

The actuator in an inverter AC is the variable frequency driver of the compressor, which usually adopts the frequency as the control signal. In the development of the MPC controller for residential ACs, the AC power consumption, rather than the AC frequency, is chosen as the variable to be optimized because most incentives (e.g., DAP and RTP) for DR are set for power shifting and power shaving. It is more straightforward to use power consumption in the objective function. The optimization result (i.e., the power of the AC), needs to be converted into frequency signals to implement DR control. The performance maps of inverter ACs can be used in an inverse manner to determine the corresponding frequency.

5. Test results and discussions

5.1. TRNSYS-MATLAB co-simulation testbed and test conditions

Computer-based dynamic simulation is usually considered an effective and reliable approach to test control performance under various conditions. Building energy simulation programs like EnergyPlus and TRNSYS are commonly used to simulate a building's thermal performance and the energy performance of its HVAC system. To take advantage of the powerful computation capabilities of

MATLAB, the steady-state AC model and the MPC controllers are programmed in MATLAB. TRNSYS and MATLAB are combined in this study, as illustrated in Fig. 9. In the integrated building energy system, the air-conditioned room is coupled with an inverter AC. The building model (Type 56) in TRNSYS is used to characterize the building's thermal performance under the influences of weather, occupancy, and AC. The output of the controller is the compressor motor's operating frequency. The inverter AC then uses the operating frequency to determine the corresponding cooling capacity and delivers it to the building component in TRNSYS. In this study, the component of Type 155 is used to establish the communication between the models in TRNSYS 18 (32-bit) and MATLAB 2014a (32-bit) in the Windows 10 64-bit operating system. The MPC controller is implemented in MATLAB using the YALMIP optimization toolbox [40] with the Gurobi optimization solver [41].

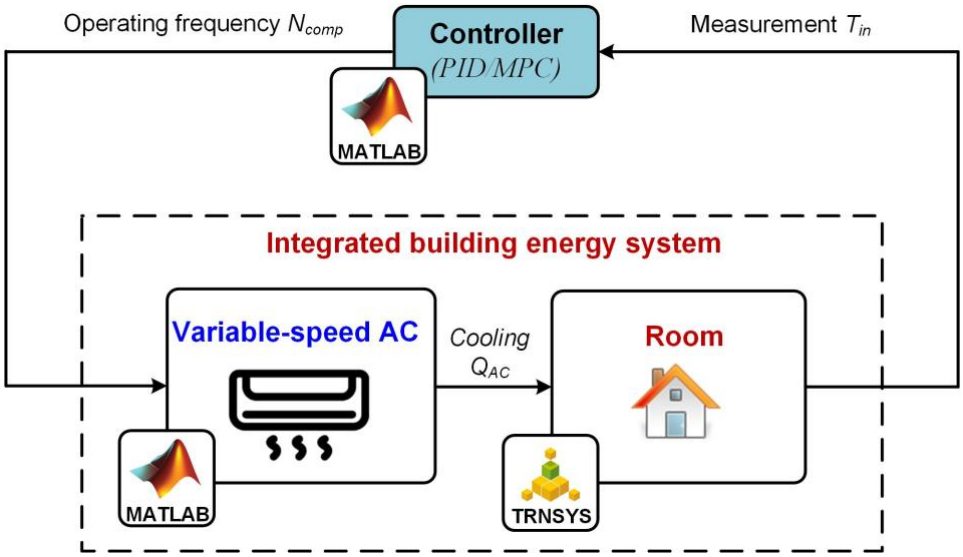

Fig. 9. TRNSYS-MATLAB co-simulation testbed for integrated building energy system.

Weather forecast data from a local observatory, occupancy profiles, and RTPs from electric utilities are the exogenous inputs of the MPC controllers. The variables for three typical summer days are shown in Fig. 10 and are used to test the performances of the MPC controllers in this study. It can be seen that RTP at 5-minute intervals from the ERCOT retail market varies throughout the day and normally reaches a peak around 16:00, which prompts DR from residential ACs. A fluctuant occupancy pattern is defined to simulate the time-changing occupancy patterns. The room is assumed to be occupied from 12:00 to 18:00 and from 20:00 to 08:00. The simulation begins at 08:00. It is

assumed that the room's thermal response is stabilized after one night of AC operation at 08:00. Thus, the AC temperature set point is used as the initial value of the indoor air temperature in the simulation.

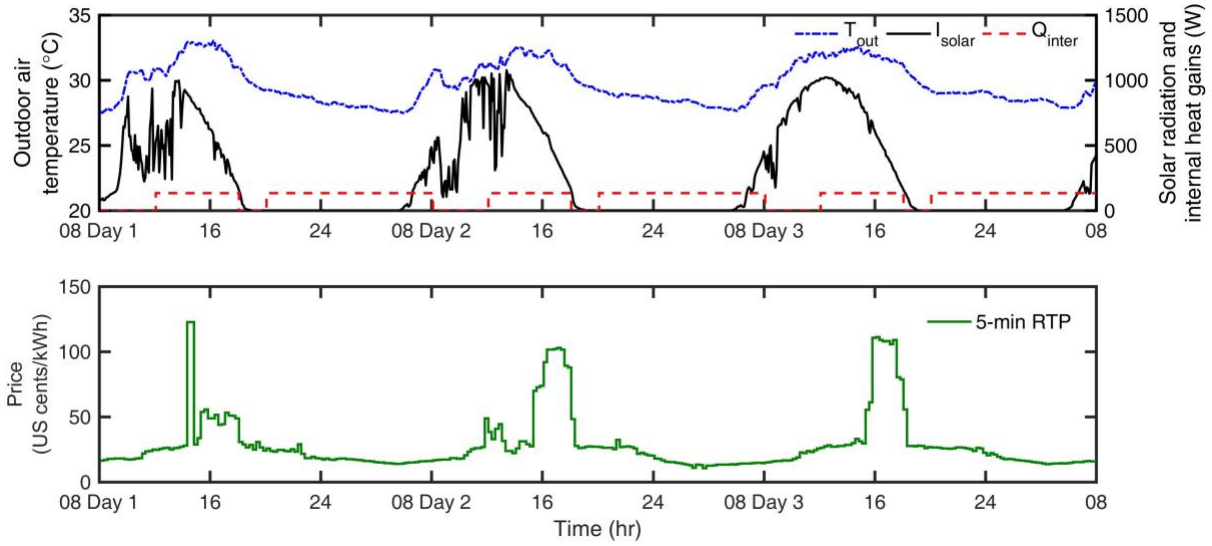

Fig. 10. Weather conditions and RTP from ERCOT on three sequential typical summer days.

5.2. Comparisons between on-off and PID control methods

System performances under on-off and PID control methods are first tested and compared. To meet the maximum cooling load of the target room, a single-speed AC with a nominal cooling capacity of 3.62 kW and a nominal COP of 2.52 is chosen. The adopted on-off control algorithm for the single-speed AC is the same as that in the baseline case of our previous study [30]. For the inverter AC, a PID controller is used to control the frequency of the inverter AC to maintain the indoor temperature at the set point. The indoor air temperature set point in both cases is 24℃ from 12:00 to 18:00 and from 20:00 to 24:00 and 26℃ from 24:00 to 08:00 to reflect the common practice of setting the indoor temperature higher at night. In this case, RTP is used only to calculate electricity costs and is not involved in the control algorithm. The simulation time step is 1 minute.

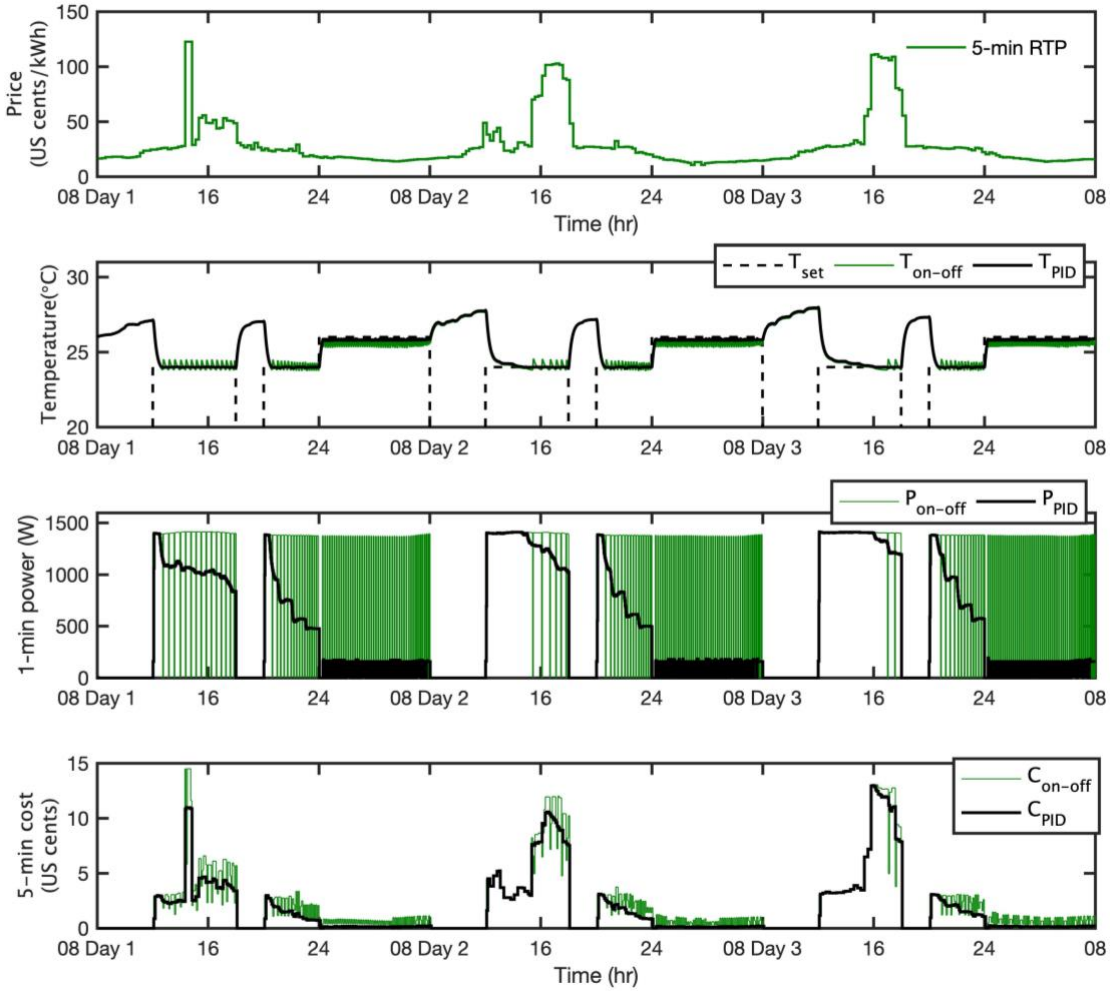

Fig. 11. (a) RTPs and system performance under on-off and PID control, including (b) indoor air temperature, (c) power consumption, and (d) electricity costs.

Fig. 11 shows the performances of the AC under on-off and PID control. As can be seen from 11-b, when the room is occupied, both the on-off and PID controller can maintain the indoor air temperature at its set point most of the time. The ACs are switched off from 18:00 to 20:00 and from 08:00 to 12:00 because it is assumed that the room is unoccupied during the periods. Compared with the single-speed AC, the inverter AC can provide a more accurate control of indoor air temperature, since it can work at low operating frequencies and supply low cooling loads when the cooling demands decrease. Besides, the inverter AC is more energy-efficient and cost-efficient than the single-speed AC. Compared with the single-speed AC, the inverter AC can provide 27.61% reduction in the total energy consumption and 16.91% reduction in total electricity cost for 3 days.

However, even using the inverter AC under PID control, the occupants still suffer from a period of thermal discomfort at the beginning of occupancy, because the inverter AC takes some time to remove

the accumulated heat gain and bring the indoor temperature to the set point. Besides, the inverter AC under PID control is not grid-friendly and cannot make response to RTPs. It can be found that the inverter AC runs at high frequencies when RTP is high around 16:00, which is a disadvantage to the power grid considering the large population of residential ACs operating at the same time. It is also a disadvantage to residential users due to the high electricity cost.

To conclude, the inverter AC with PID control is more energy-efficient and cost-efficient than the single-speed AC with on-off control, but it is not grid-interactive and cannot provide energy flexibility for grids. The present study focuses on the inverter AC, and the case under PID control is regarded as a reference case and will be compared with the following MPC cases.

5.3. Comparisons between reference case and MPC cases

The simulation tests with the two types of MPC controllers are conducted separately under conditions identical to those used in the reference case (PID case). The simulation time step in TRNSYS is set as 5 minutes, and at each time step the MPC controller in MATLAB is called by TRNSYS, and the frequency control signal is sent to the inverter AC model.

5.3.1. Ordinary MPC controller without DR function

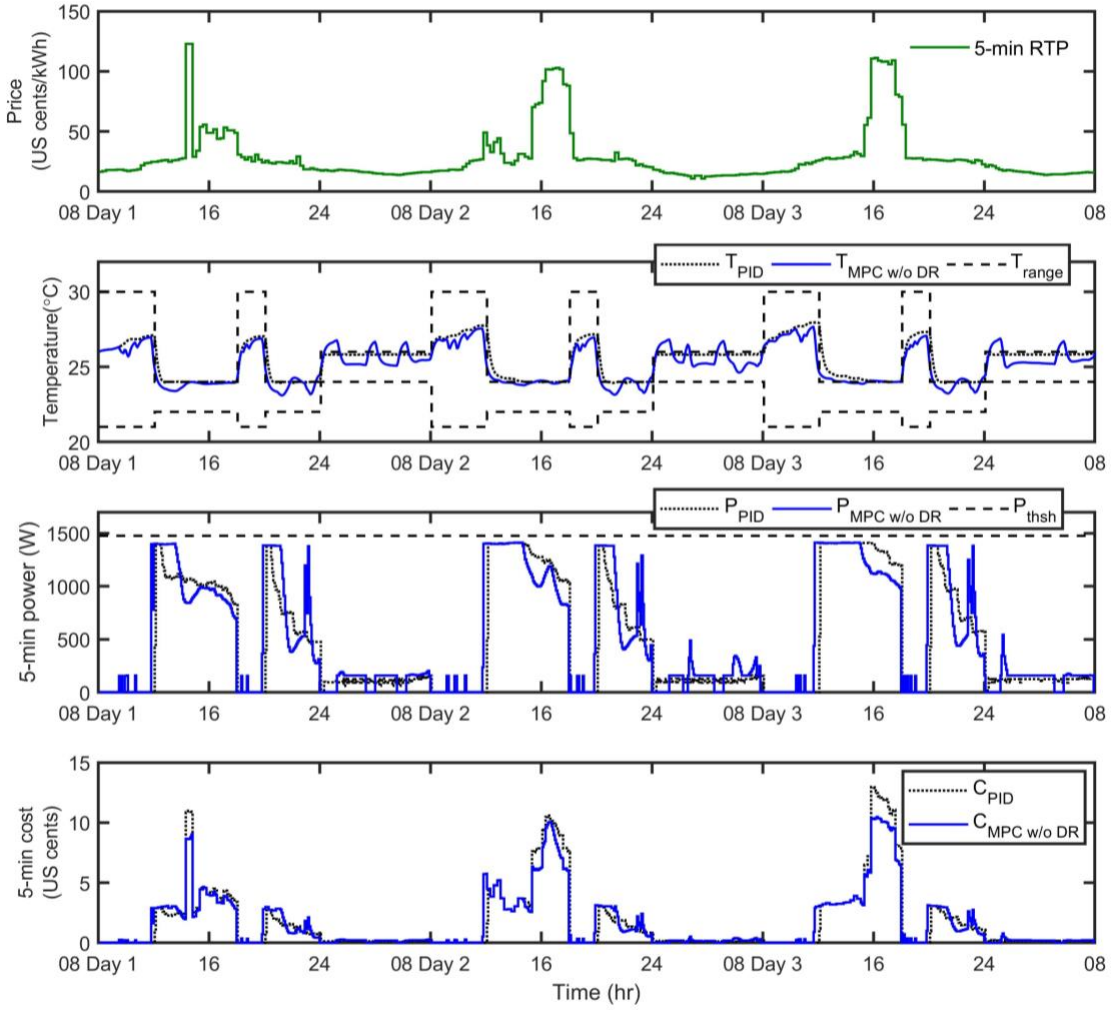

Fig. 12. (a) RTPs and system performance under PID control and ordinary MPC without DR function, including (b) indoor air temperature, (c) power consumption, and (d) electricity costs.

Fig. 12 shows the system performances under the ordinary MPC without DR function. For easy comparison, the RTP and the performances under the PID control are shown in the same figure. Fig. 12-b shows that the MPC controller, as a new optimal control method for inverter ACs, satisfactorily maintains the indoor air temperature between the upper and lower limits, although the temperature fluctuates due to the uncertain noise. The results also show that the ordinary MPC controller naturally implements the precooling strategy, which obviously improves thermal comfort at the beginning of occupancy. On Day 1, the prediction made by the MPC controller at 10:00 indicates that the indoor air temperature will exceed the upper boundary (i.e., 24°C) at 12:00. Hence, the inverter AC begins to run at 10:00 to precool the room before it is occupied so that the indoor air temperature is at a comfortable level at the beginning of occupancy. In the PID case, the temperature deviations from the

set point evaluated by the mean absolute error (MAE) from 12:00 to 14:00 are 0.39℃, 0.78℃, and 0.96℃ on Days 1, 2 and 3, respectively, which are greater than those in the MPC case (i.e., 0.06°C, 0.17°C, and 0.18°C, respectively). Moreover, precooling is an optimal solution because the objective of the ordinary MPC is to minimize the energy consumption in the horizon. The ordinary MPC controller automatically implements precooling with different start-up times and durations on the three days because the weather conditions differ. In this way, the ordinary MPC controller solves the problem of determining the start-up time for precooling, which was challenging for most previous studies in which a precooling strategy was developed [42, 43]. Precooling may result in an increase in energy consumption, which can be observed in the test results shown in Fig. 14-b. The AC under the ordinary MPC control consumes more energy than that under the PID control on these three days. However, the daily operating costs may be reduced, as shown in Fig. 14-d, because the MPC controller allows a higher indoor air temperature than the PID controller.

5.3.2. DR-enabled MPC controller responding to RTP

The DR-enabled MPC controller considers the RTP in the optimization process. Dynamic power thresholds can be generated using Eq. (16) according to the RTP signals from the electric utility. The dynamic power threshold acts as a time-varying constraint in the solution of the optimization problem.

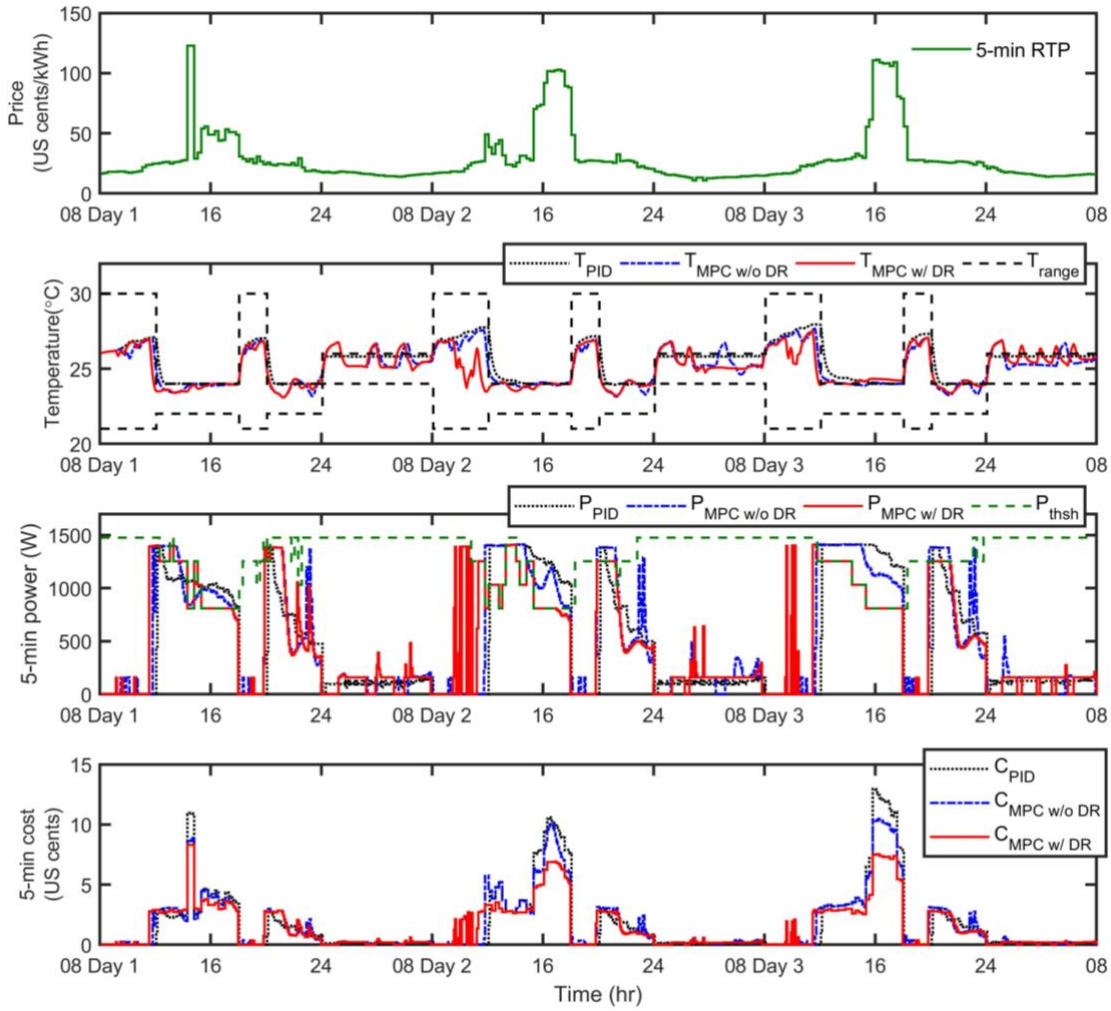

Fig. 13. (a) RTPs and system performances under PID control, ordinary MPC without DR function, and DR-enabled MPC, including (b) indoor air temperature, (c) power consumption, and (d) electricity costs.

Fig. 13 shows the system performances under the PID control, the ordinary MPC without DR function, and the DR-enabled MPC. Like the ordinary MPC controller without DR function, the DR-enabled MPC controller can implement automatic and optimal precooling. However, the DR-enabled MPC controller adopts longer and deeper precooling to limit power consumption during peak demand periods. It starts the inverter AC to precool the room to a lower temperature so that the AC power consumption and operating frequency can be limited around 16:00, when the RTP is very high. Thermal comfort can be maintained due to the cooling energy stored in the thermal mass during the precooling period. As can be seen from Fig. 14-c, compared with the PID case, that the average power consumption from 15:00 to 17:00 is reduced by 17.31% on Day 1, 31.00% on Day 2, and 38.86% on Day 3, in the DR-enabled MPC control case. Because the DR-enabled MPC controller effectively shifts power consumption from high-RTP periods to low-RTP periods, the all-day electricity costs are

reduced by 0.42% on Day 1, 13.75% on Day 2, and 22.16% on Day 3. The electricity cost saving is influenced by the weather conditions and RTP profiles. For example, the weather on Day 1 is cooler than that on Days 2 and 3 and the RTP curve is flatter, so the electricity cost saving is less. Meanwhile, as shown by Fig. 14-b, the daily energy consumption of the AC under the DR-enabled MPC may exceed that under the PID control. This is the price paid to achieve power reductions during the peak demand hours via precooling. From the prospective of power grids, it is more important to provide a stable power reduction as required.

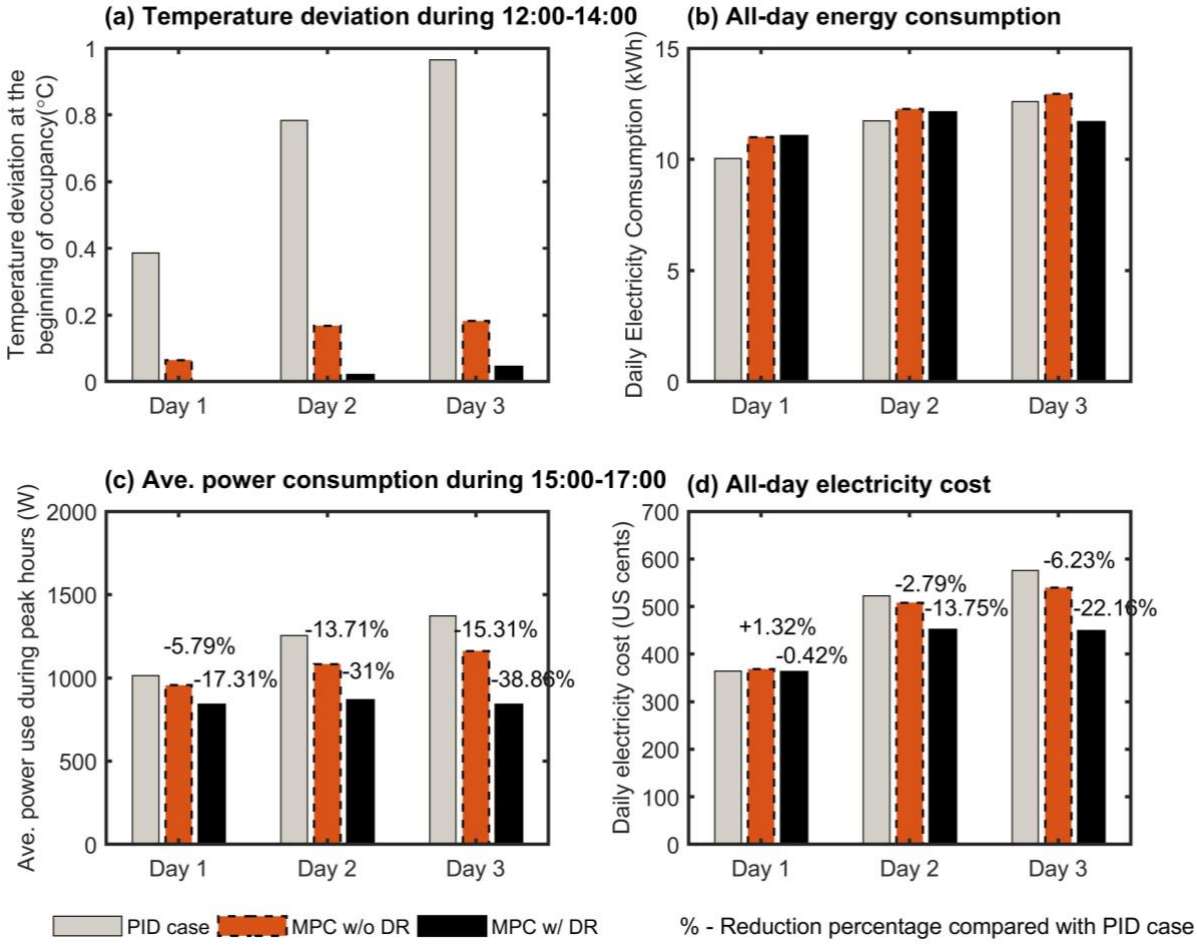

Fig. 14. System performances under PID control, ordinary MPC without DR function, and DR-enabled MPC.

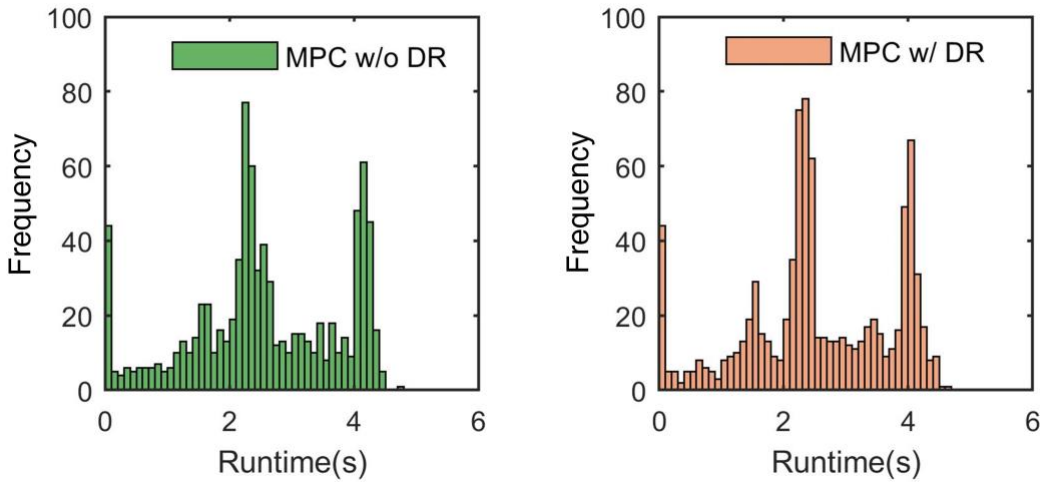

Fig. 15. Frequency distribution of computation time of the ordinary MPC controller without DR function (left) and the DR-enabled MPC controller (right) at each time step.

Fig. 15 shows the computation time required to solve the optimization problem at each time step using a PC with Intel Core i7-4600U 2.70 GHz. The computation time is less than 5 seconds, which is shorter than the prediction interval of 5 minutes. Therefore, the MPC controllers are competent in real-time online control.

6. Conclusions

In this study, we propose an advanced demand response-enabled model predictive control method to directly control the operating frequency of inverter air conditioners in response to 5-min real-time electricity prices, which is largely different from most of the previous demand response control methods that focus on single-speed air conditioners and respond to hourly day ahead electricity prices by resetting indoor air temperature set points.

The test results show that, compared with the PID controller, the demand response-enabled model predictive controller can reduce the power consumption during peak demand periods by 17.31% to 38.86% and reduce all-day electricity costs by 0.42% to 22.16%. The percentages of peak power reduction and cost savings are influenced by the room's thermal mass, the weather conditions, and the real-time electricity prices. The total energy consumption of inverter air conditioners under the model predictive control may exceed that under PID control because the model predictive controller adopts precooling to shift power demands during peak demand periods. The thermal comfort at the beginning of occupancy under the model predictive control is improved by automatic precooling. The

test results also show that the computation time of the model predictive controllers is suitable for online real-time control.

Due to the simple structure and moderate computation time, both the simplified room thermal model and the performance maps of inverter air conditioner can be used in smart home energy management system for model-based optimal control to reduce electricity bills. The simplified models can also be used by grid operators to investigate the demand response potential of a large population of air conditioners. Demand curve flattening achieved by the proposed control method can provide financial benefits to the grid operators. It can help to avoid additional generation capacity and the upgrade of distribution and transmission infrastructure considering the great contribution of power reduction from a huge number of residential air conditioners. Moreover, since the operating frequency of compressor is closely related to the power consumption of inverter air conditioners, the frequency-based control method can provide fast demand response, maintain the grid operating frequency, and improve the grid reliability.

Acknowledgement

The research work presented in this paper is financially supported by a research grant (G-YBTB) in the Hong Kong Polytechnic University (PolyU) and the Strategic Focus Area (SFA) Scheme (1-BBW7) of Research Institute for Sustainable Urban Development (RISUD) in PolyU. The support is gratefully acknowledged.

References

[1] Federal Energy Regulatory Commission. National action plan on demand response. 2010.

[2] Federal Energy Regulatory Commission. A national assessment of demand response potential. 2009.

[3] Chen Z, Wu L, Fu Y. Real-time price-based demand response management for residential appliances via stochastic optimization and robust optimization. Smart grid, IEEE transactions on. 2012;3:1822-31.

[4] Hubert T, Grijalva S. Modeling for residential electricity optimization in dynamic pricing environments. Smart Grid, IEEE Transactions on. 2012;3:2224-31.

[5] Li S, Zhang D, Roget AB, O'Neill Z. Integrating home energy simulation and dynamic electricity price for demand response study. Smart Grid, IEEE Transactions on. 2014;5:779-88.

[6] Thomas AG, Jahangiri P, Wu D, Cai C, Zhao H, Aliprantis DC, et al. Intelligent residential air-conditioning system with smart-grid functionality. Smart Grid, IEEE Transactions on. 2012;3:2240-51.

[7] Modiri-Delshad M, Aghay Kaboli SH, Taslimi-Renani E, Rahim NA. Backtracking search algorithm for solving economic dispatch problems with valve-point effects and multiple fuel options. Energy. 2016;116:637-49.

[8] Kaboli SHA, Selvaraj J, Rahim NA. Long-term electric energy consumption forecasting via artificial cooperative search algorithm. Energy. 2016;115:857-71.

[9] Kaboli SHA, Fallahpour A, Selvaraj J, Rahim NA. Long-term electrical energy consumption formulating and forecasting via optimized gene expression programming. Energy. 2017;126:144-64.

[10] Aswani A, Master N, Taneja J, Culler D, Tomlin C. Reducing transient and steady state electricity consumption in HVAC using learning-based model-predictive control. Proceedings of the IEEE. 2012;100:240-53.

[11] Federal Energy Regulatory Commission. Assessment of demand response and advanced metering. 2018.

[12] Qin SJ, Badgwell TA. A survey of industrial model predictive control technology. Control Engineering Practice. 2003;11:733-64.

[13] Široký J, Oldewurtel F, Cigler J, Prívara S. Experimental analysis of model predictive control for an energy efficient building heating system. Applied Energy. 2011;88:3079-87.

[14] Khanmirza E, Esmaeilzadeh A, Markazi AHD. Design and experimental evaluation of model predictive control vs. intelligent methods for domestic heating systems. Energy and Buildings. 2017;150:52-70.

[15] O'Dwyer E, De Tommasi L, Kouramas K, Cychowski M, Lightbody G. Modelling and disturbance estimation for model predictive control in building heating systems. Energy and Buildings. 2016;130:532-45.

[16] Oldewurtel F, Parisio A, Jones CN, Gyalistras D, Gwerder M, Stauch V, et al. Use of model predictive control and weather forecasts for energy efficient building climate control. Energy and Buildings. 2012;45:15-27.

[17] Moroşan P-D, Bourdais R, Dumur D, Buisson J. Building temperature regulation using a distributed model predictive control. Energy and Buildings. 2010;42:1445-52.

[18] Álvarez JD, Redondo JL, Camponogara E, Normey-Rico J, Berenguel M, Ortigosa PM. Optimizing building comfort temperature regulation via model predictive control. Energy and Buildings. 2013;57:361-72.

[19] Chen X, Wang Q, Srebric J. Model predictive control for indoor thermal comfort and energy optimization using occupant feedback. Energy and Buildings. 2015;102:357-69.

[20] Hedegaard RE, Pedersen TH, Petersen S. Multi-market demand response using economic model predictive control of space heating in residential buildings. Energy and Buildings. 2017;150:253-61.

[21] Rawlings JB, Patel NR, Risbeck MJ, Maravelias CT, Wenzel MJ, Turney RD. Economic MPC and real-time decision making with application to large-scale HVAC energy systems. Computers & Chemical Engineering. 2018;114:89-98.

[22] Dahl Knudsen M, Petersen S. Demand response potential of model predictive control of space heating based on price and carbon dioxide intensity signals. Energy and Buildings. 2016;125:196-204.

[23] Oldewurtel F, Ulbig A, Parisio A, Andersson G, Morari M. Reducing peak electricity demand in building climate control using real-time pricing and model predictive control. Decision and Control (CDC), 2010 49th IEEE Conference on: IEEE; 2010. p. 1927-32.

[24] Ma J, Qin J, Salsbury T, Xu P. Demand reduction in building energy systems based on economic model predictive control. Chemical Engineering Science. 2012;67:92-100.

[25] Wanjiru EM, Sichilalu SM, Xia X. Model predictive control of heat pump water heater-instantaneous shower powered with integrated renewable-grid energy systems. Applied Energy. 2017;204:1333-46.

[26] Sultana WR, Sahoo SK, Sukchai S, Yamuna S, Venkatesh D. A review on state of art development of model predictive control for renewable energy applications. Renewable and Sustainable Energy Reviews. 2017;76:391-406.

[27] Hu M, Xiao F. Price-responsive model-based optimal demand response control of inverter air conditioners using genetic algorithm. Applied Energy. 2018;219:151-64.

[28] Zhu Y. Multivariable system identification for process control: Elsevier; 2001.

[29] Cigler J, Gyalistras D, Široky J, Tiet V, Ferkl L. Beyond theory: the challenge of implementing model predictive control in buildings. Proceedings of 11th Rehva world congress, Clima2013.

[30] Hu M, Xiao F, Wang L. Investigation of demand response potentials of residential air conditioners in smart grids using grey-box room thermal model. Applied Energy. 2017;207:324-35.

[31] Zhou Q, Wang S, Xu X, Xiao F. A grey-box model of next-day building thermal load prediction for energy-efficient control. International Journal of Energy Research. 2008;32:1418-31.

[32] Zhou B, Li W, Chan KW, Cao Y, Kuang Y, Liu X, et al. Smart home energy management systems: Concept, configurations, and scheduling strategies. Renewable and Sustainable Energy Reviews. 2016;61:30-40.

[33] Electricity Reliability Council Of Texas (ERCOT). Historical RTM Load Zone and Hub Prices. Available from http://misercotcom/misapp/GetReportsdo?reportTypeId=13061&reportTitle=Historical%20RTM%20Load%20Zone%20and%20Hub%20Prices&showHTMLView=&mimicKey. 2017.

[34] Feng JD, Chuang F, Borrelli F, Bauman F. Model predictive control of radiant slab systems with evaporative cooling sources. Energy and Buildings. 2015;87:199-210.

[35] Halvgaard R, Poulsen NK, Madsen H, Jørgensen JB. Economic model predictive control for building climate control in a smart grid. Innovative Smart Grid Technologies (ISGT), 2012 IEEE PES: IEEE; 2012. p. 1-6.

[36] Hedegaard RE, Pedersen TH, Knudsen MD, Petersen S. Towards practical model predictive control of residential space heating: Eliminating the need for weather measurements. Energy and Buildings. 2018;170:206-16.

[37] Karlsson H, Hagentoft C-E. Application of model based predictive control for water-based floor heating in low energy residential buildings. Building and Environment. 2011;46:556-69.

[38] Bishop G, Welch G. An introduction to the Kalman filter. Proc of SIGGRAPH, Course. 2001;8:41.

[39] Simon D. Optimal state estimation: Kalman, H infinity, and nonlinear approaches: John Wiley & Sons; 2006.

[40] Löfberg J. YALMIP: A toolbox for modeling and optimization in MATLAB. Computer Aided Control Systems Design, 2004 IEEE International Symposium on: IEEE; 2004. p. 284-9.

[41] Gurobi Optimization I. Gurobi optimizer reference manual. URL http://wwwgurobicom. 2016.

[42] Sun Y, Wang S, Xiao F, Huang G. A study of pre-cooling impacts on peak demand limiting in commercial buildings. HVAC&R Research. 2012;18:1098-111.

[43] Turner WJN, Walker IS, Roux J. Peak load reductions: Electric load shifting with mechanical pre-cooling of residential buildings with low thermal mass. Energy. 2015;82:1057-67.